Supplemental Information

Supplemental Table Legends

Table S1 **Summary of RNA-sequencing results**

Table S2 **Lists of genes whose transcripts' decay followed first-order kinetics with no knockdown or knockdown of either Pan3L, Pan3S, or both isoforms.**

Table S3 **A list of genes whose transcripts' decay followed first-order kinetics under all knockdown conditions.**

Supplemental Figure Legends

Figure S1. Pan3L and Pan3S isoforms are conserved among warm-blooded vertebrates. Pan3 protein sequences were downloaded from the NCBI database. Multiple alignment was performed by ClustalX (v2.1) with manual check.

Figure S2. The two Pan3 isoforms exhibit different interaction strengths with PABP in human BEAS-2B cells. Co-immunoprecipitation (Co-IP) and Western blot analyses showing that HA-Pan3S pulls down more endogenous PABP than HA-Pan3L does, whereas the two Pan3 isoforms pull down similar amounts of endogenous Pan2 (**A**), and that HA-Pan3L and HA-Pan3S exhibit a similar ability to interact with Pan2-V5 (**B**). GAPDH served as the negative control for co-IP. The amount of each "Input" sample loaded onto the gel was 5% (**A)** or 3% (**B**) of the amount of the corresponding lysate used for IP.

Figure S3. Effects of Pan3 domain truncations on Pan3-PABP and Pan3-Pan2 interactions in human BEAS-2B cells. Co-immunoprecipitation (Co-IP) and Western blot analyses showing the effects of Pan3 domain truncations on HA-Pan3 isoforms' abilities to pull down endogenous PABP and Pan2. Refer to Fig. 2A for the schematic diagram of Pan3 isoform mutants and their nomenclature. Note that when either one of the three domains was truncated (ΔN, ΔK, or ΔC), the ability of Pan3 to interact with PABP and Pan2 was appreciably reduced. GAPDH served as the negative control for co-IP. The amount of each "Input" sample loaded onto the gel was 5% of the amount of the corresponding lysate used for IP.

Figure S4. Setting up a cell-based deadenylation assay to test the effects of the two Pan3 isoforms on Pan2 deadenylase activity *in vivo*. NIH3T3 cells were transiently transfected with plasmid(s) expressing the indicated HA-tagged proteins. To optimize testing conditions, different amounts of HA-Pan2 were expressed either alone or together with a fixed amount of one of the HA-tagged Pan3 isoforms. β-globin mRNA constitutively expressed in the same cells was used as the reporter transcript. **A**: Northern blot showing poly(A) size distribution of β-globin reporter mRNA. Poly(A)$^-$ RNA sample was prepared with oligo(dT) and RNase H treatment. **B**: Western blot showing the levels of the indicated HA-tagged proteins; GAPDH served as the loading control. **C**: Poly(A) size distribution profiles obtained by scanning each lane of the Northern blot shown in A, using ImageJ software. Red arrows (**A** and **C**) highlight changes of the profile caused by expression of HA-Pan2 with or without co-expression of the HA-Pan3 isoforms.

Figure S5. Pan3L and Pan3S have different effects on Pan2 deadenylase activity in human BEAS-2B cells. Northern blot (upper panel) showing effects of ectopic expression of HA-Pan2 with and without individual Pan3 isoforms on poly(A) size distribution of constitutively expressed β–globin reporter mRNA. Poly(A)$^-$ RNA samples (A$^-$) were prepared with oligo(dT) and RNase H treatment. Levels of HA-Pan2 and HA-Pan3 isoforms proteins were assessed by Western blot analysis (lower panel); GAPDH served as loading control. The poly(A) size distribution profiles (upper right) were obtained by scanning each lane of the Northern blots using ImageJ software. Red brackets highlight changes of the profile caused by expression of HA-Pan2 with and without co-expression of HA-Pan3 isoforms.

Figure S6. Pan3L and Pan3S knockdowns exhibit differential effects on P-body abundance in Human BEAS-2B cells. BEAS-2B cells were transfected with control siRNA (control KD), Pan3L-specific siRNA (Pan3L KD), Pan3S-specific siRNA (Pan3S KD), or both Pan3 siRNAs (Pan3S+L KD). Immunofluorescence microscopy was used to visualize markers for total P-bodies (TNRC6 in **A** and Dcp1a in **B**; green or Rck/p54 in **A**; red) or for GW/P-bodies (GW220 in **B**; red). RT-PCR and gel-electrophoresis were used to assess the Pan3 knockdown efficiency; GAPDH served as the loading control.

Figure S7. Bioinformatics analysis of miRNA-binding site enrichment across the transcriptome under the conditions of depleting individual or both Pan3 isoforms. The miRNA target sites for each transcript were predicted using the starBase platform (http://starbase.sysu.edu.cn/) (Li et al. 2014), which takes into account the Ago-CLIP-seq data sets. The miRNA-binding sites included in the analysis have been associated with an Ago protein in at least three separate Ago-CLIP-seq experiments, and the cognate miRNA must express in U2OS cells at a moderate level of at least 5,000 counts (Mayr and Bartel 2009). The values shown are the predicted average numbers of miRNA-binding sites in the 3"UTR of transcripts that are stabilized (fold change >1) or non-stabilized (fold change $\leqslant$1) by Pan3L knockdown (**A**), Pan3S knockdown (**B**) or combined Pan3 isoforms knockdown (**C**). Wilcox test was performed for the significance between the two groups under different Pan3 isoform knockdown conditions.

Figure S8. GATHER (http://gather.genome.duke.edu/) analysis results showing the enriched Gene Ontology terms, enriched transcription factor-binding sites (TRANSFAC), and potential

participated cellular pathways (KEGG Pathway) of the genes whose transcripts were stabilized by at least 3 fold upon knockdown of Pan3S (**A**) or both isoforms (**B**).

Figure S9. A model illustrating how the first phase of deadenylation may be coordinated by the concerted action of Pan2, PABP, Pan3L and Pan3S. Refer to the Discussion for details. Note that for simplicity purpose, Pan2-Pan3L shuttling between the nucleus and cytoplasm is not depicted.

Figure S10. Immunofluorescence microscopy results showing the nucleo-cytoplasmic distribution of HA-Pan3L and HA-Pan3S in U2OS cells. Leptomycin B treatment (20 ng/ml) for 4h resulted in nuclear accumulation of HA-Pan3L but had no effect on the distribution of HA-Pan3S, which remained in the cytoplasm. HA-tagged Pan3 isoforms were detected using rat anti-HA monoclonal antibody and Alexa Fluor 350 (Green) conjugated to goat anti-rat IgG. Nuclei were identified by DAPI staining (blue). Bars represent 50 μm.

References:

Li J-H, Liu S, Zhou H, Qu L-H, Yang J-H. 2014. starBase v2.0: decoding miRNA-ceRNA, miRNA-ncRNA and protein,ÄìRNA interaction networks from large-scale CLIP-Seq data. *Nucleic Acids Research* **42**: D92-D97.

Mayr C, Bartel DP. 2009. Widespread Shortening of 3'UTRs by Alternative Cleavage and Polyadenylation Activates Oncogenes in Cancer Cells. *Cell* **138**: 673-684.

The L- and S-isoforms of Pan3 are conserved in warm-blooded vertebrates.

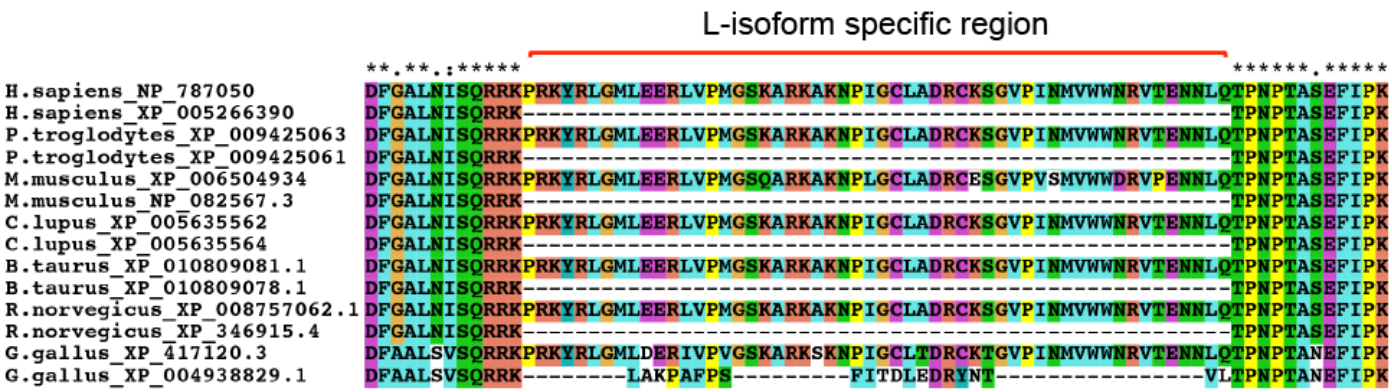

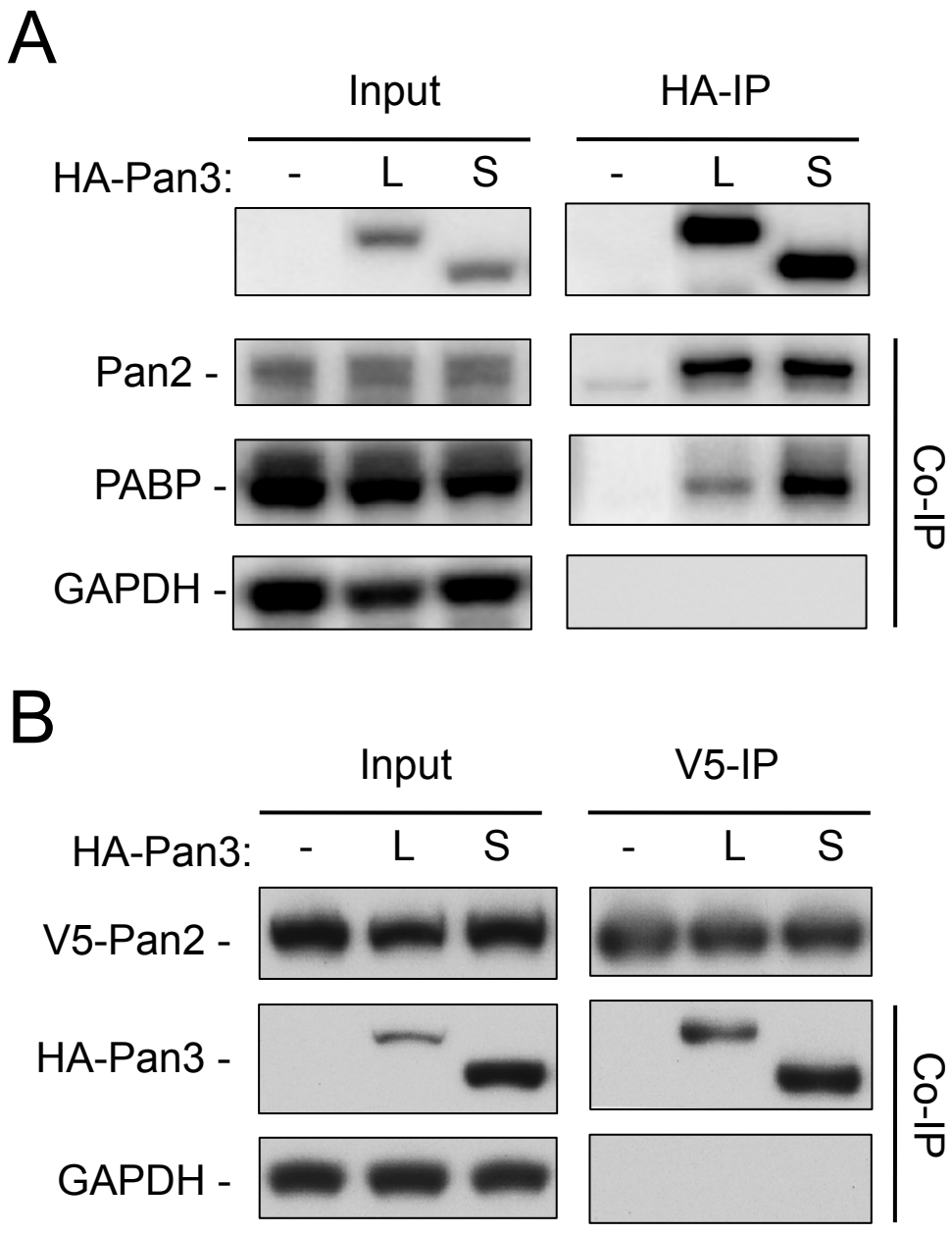
A
Input
HA-IP
HA-Pan3:
-
L
S
-
L
S
Pan2 -
PABP -
GAPDH -
Co-IP
B
Input
V5-IP
HA-Pan3:
-
L
S
-
L
S
V5-Pan2 -
HA-Pan3 -
GAPDH -
Co-IP

Shyu Figure S3

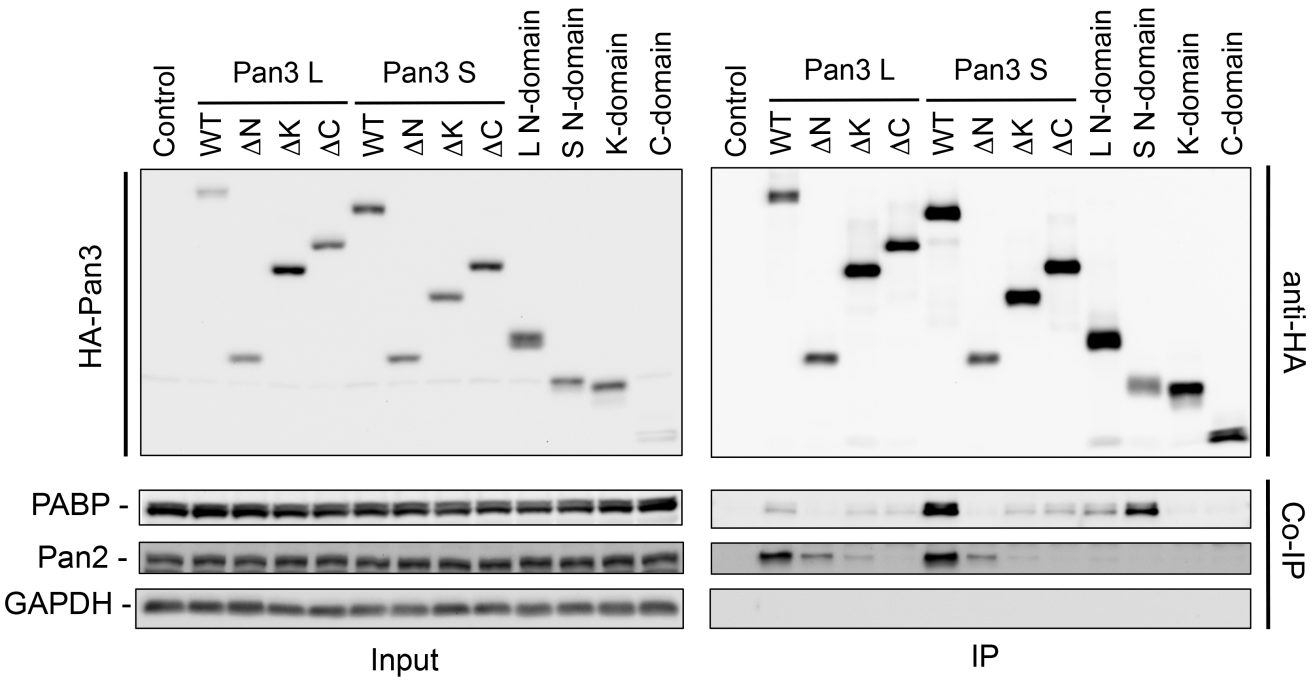

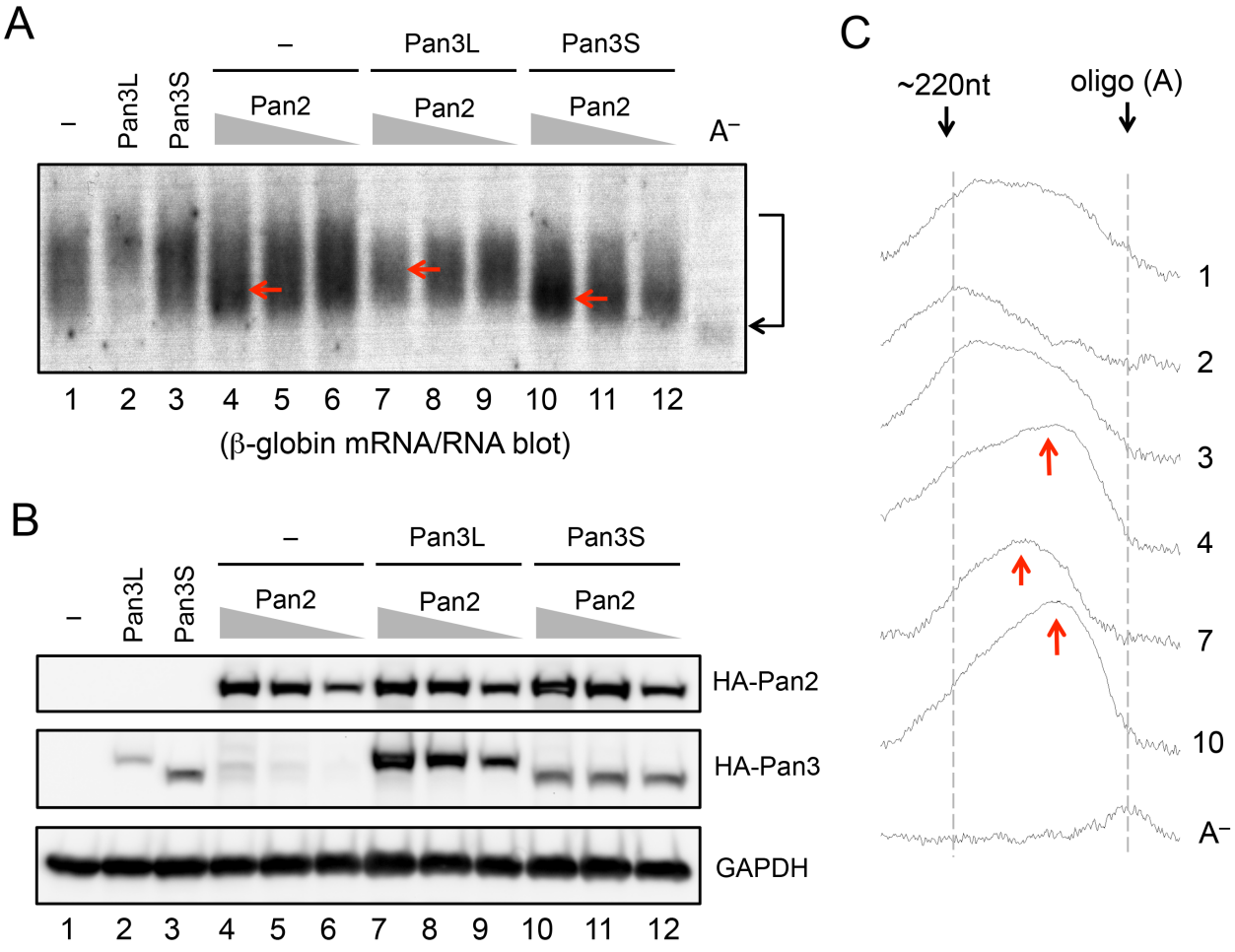
A
–
Pan3L
Pan3S
–
Pan3L
Pan3S
Pan2
Pan2
Pan2
A⁻
1 2 3 4 5 6 7 8 9 10 11 12
(β-globin mRNA/RNA blot)
B
–
Pan3L
Pan3S
–
Pan3L
Pan3S
Pan2
Pan2
Pan2
HA-Pan2
HA-Pan3
GAPDH
1 2 3 4 5 6 7 8 9 10 11 12
C
~220nt
oligo (A)
1
2
3
4
7
10
A⁻

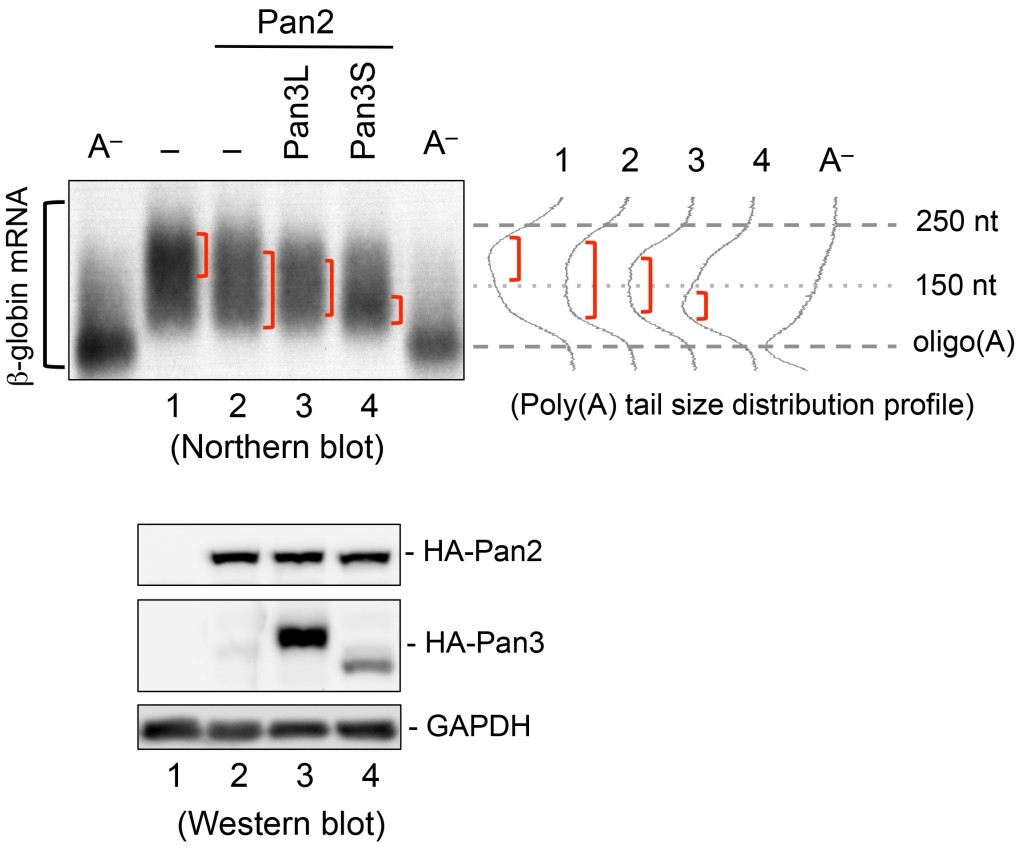
Pan2
Pan3L
Pan3S
A⁻
–
–
A⁻
β-globin mRNA
1 2 3 4
(Northern blot)
1 2 3 4 A⁻
250 nt
150 nt
oligo(A)
(Poly(A) tail size distribution profile)
- HA-Pan2
- HA-Pan3
- GAPDH
1 2 3 4
(Western blot)

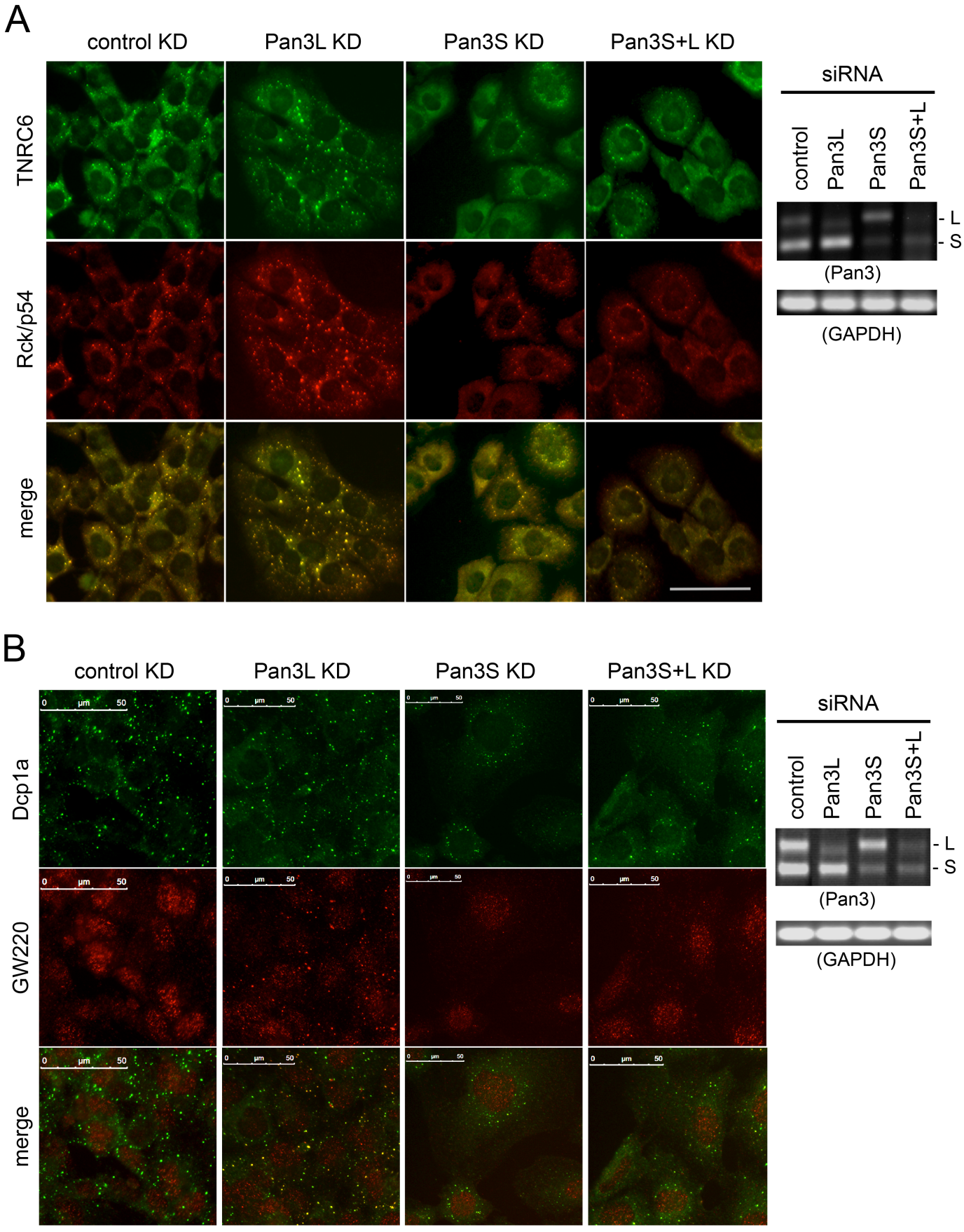
A
control KD
Pan3L KD
Pan3S KD
Pan3S+L KD
TNRC6
Rck/p54
merge
siRNA
control
Pan3L
Pan3S
Pan3S+L
- L
- S
(Pan3)
(GAPDH)
B
control KD
Pan3L KD
Pan3S KD
Pan3S+L KD
Dcp1a
GW220
merge
siRNA
control
Pan3L
Pan3S
Pan3S+L
- L
- S
(Pan3)
(GAPDH)

A

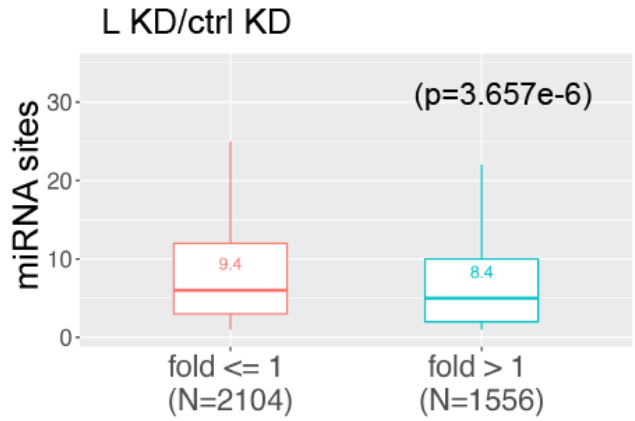
L KD/ctrl KD
(p=3.657e-6)
miRNA sites
30
20
10
0
9.4
8.4
fold <= 1
(N=2104)
fold > 1
(N=1556)

B

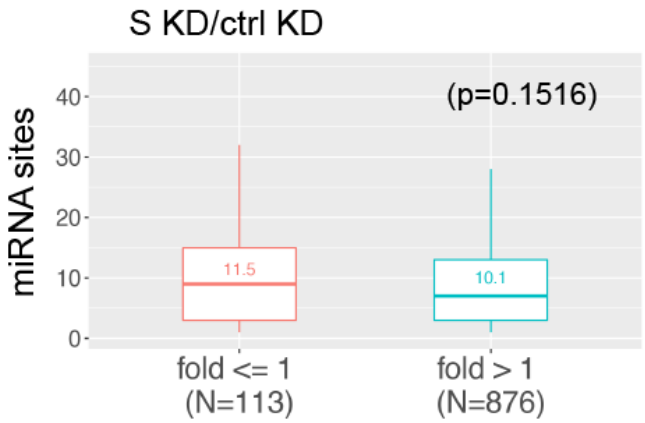
S KD/ctrl KD
(p=0.1516)
miRNA sites
40
30
20
10
0
11.5
10.1
fold <= 1
(N=113)
fold > 1
(N=876)

C

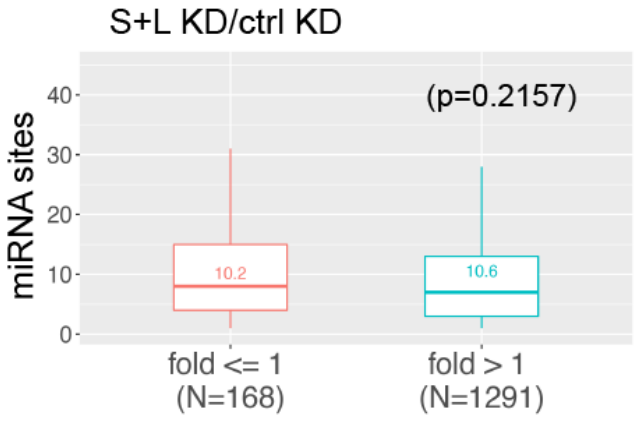
S+L KD/ctrl KD
(p=0.2157)
miRNA sites
40
30
20
10
0
10.2
10.6
fold <= 1
(N=168)
fold > 1
(N=1291)

A Pan3S knockdown

Gene Ontology	# Genes	p Value	Bayes Factor
1. GO:0006139 [5]: nucleobase, nucleoside, nucleotide and nu...	138 [show]	< 0.0001	28
2. GO:0044238 [4]: primary metabolism	219 [show]	< 0.0001	21
3. GO:0044237 [4]: cellular metabolism	223 [show]	< 0.0001	18

TRANSFAC	# Genes	p Value	Bayes Factor
1. V$E2F1_Q6: E2F-1	329 [show]	< 0.0001	27
2. V$E2F1_Q3_01	248 [show]	< 0.0001	23
3. V$E2F1_Q6_01	261 [show]	< 0.0001	22
4. V$E2F_Q6: E2F	363 [show]	< 0.0001	22
5. V$E2F_Q3_01	247 [show]	< 0.0001	18

KEGG Pathway	# Genes	p Value	Bayes Factor
1. path:hsa04120: Ubiquitin mediated proteolysis	5 [show]	0.003	2
2. path:hsa04110: Cell cycle	7 [show]	0.006	1
3. path:hsa04010: MAPK signaling pathway	12 [show]	0.006	1
4. path:hsa04520: Adherens junction	6 [show]	0.007	1

B Pan3S+L knockdown

Gene Ontology	# Genes	p Value	Bayes Factor
1. GO:0006139 [5]: nucleobase, nucleoside, nucleotide and nu...	183 [show]	< 0.0001	38
2. GO:0050875 [3]: cellular physiological process	370 [show]	< 0.0001	27
3. GO:0044238 [4]: primary metabolism	287 [show]	< 0.0001	26
4. GO:0044237 [4]: cellular metabolism	294 [show]	< 0.0001	24
5. GO:0050874 [3]: organismal physiological process	18 [show]	< 0.0001	22
6. GO:0007049 [5]: cell cycle	62 [show]	< 0.0001	21

TRANSFAC	# Genes	p Value	Bayes Factor
1. V$E2F1_Q6: E2F-1	447 [show]	< 0.0001	33
2. V$E2F1_Q3_01	320 [show]	< 0.0001	19
3. V$KROX_Q6	361 [show]	< 0.0001	17
4. V$E2F_Q3_01	322 [show]	< 0.0001	15
5. V$E2F1_Q6_01	331 [show]	< 0.0001	14

KEGG Pathway	# Genes	p Value	Bayes Factor
1. path:hsa04110: Cell cycle	17 [show]	< 0.0001	13
2. path:hsa04010: MAPK signaling pathway	22 [show]	< 0.0001	7
3. path:hsa00240: Pyrimidine metabolism	10 [show]	0.001	3

Shyu Figure S9

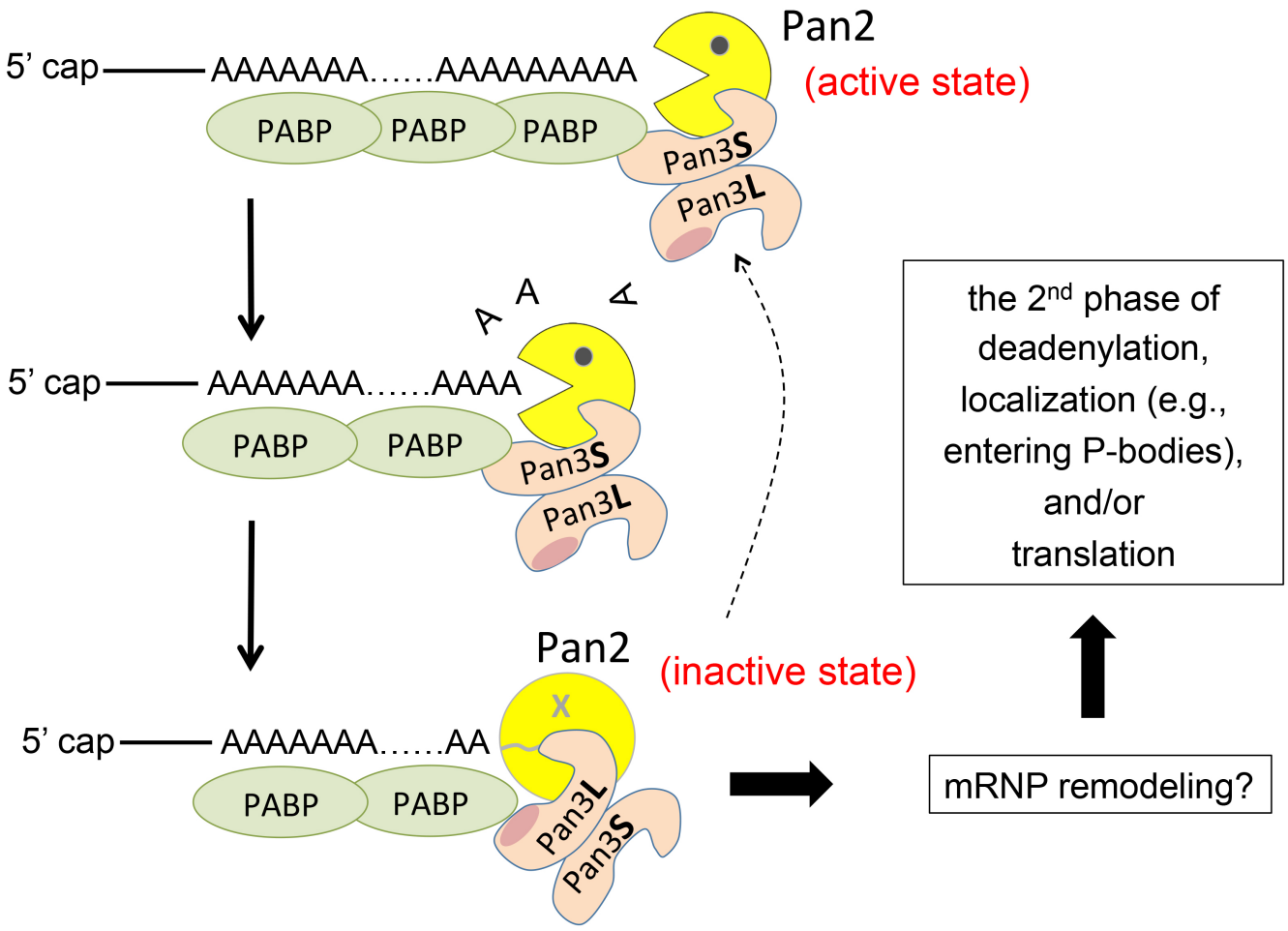

Shyu Figure S10